Published in final edited form as:
J Parasitol. 2008 December ; 94(6): 1225–1232. doi:10.1645/GE-1411.1.

CRYPTOSPORIDIUM INFECTION CAUSES UNDERNUTRITION AND, CONVERSELY, WEANLING UNDERNUTRITION INTENSIFIES INFECTION

Bruna P. Coutinho, **Reinaldo B. Oriá**, **Carlos M. G. Vieira**, **Jesus Emmanuel A. D. Sevilleja**, **Cirle A. Warren**, **Jamilly G. Maciel**, **Meghan R. Thompson**, **Relana C. Pinkerton**, **Aldo A. M. Lima**, and **Richard L. Guerrant***
Center for Global Health, School of Medicine, University of Virginia, MR4, Lane Road, Room 3148, P.O. Box 801379, Charlottesville, Virginia 22908

Abstract

Cryptosporidium parvum is a leading pathogen in children in developing countries. To investigate whether early postnatal malnutrition leads to heavier *C. parvum* infections, we assessed intestinal adaptation and parasite load in suckling mice during the first 2 wk of life, analogous to the first postnatal yr in humans. Undernutrition was induced by daily C57BL6J pup separation from lactating dams. Half of the pups were separated daily, for 4 hr on day 4, 8 hr on day 5, and for 12 hr from day 6 until day 14. On day 6, each pup received an oral inoculum of 10^5 to 10^7 parasites in 10–25 μl of PBS. Littermate controls received PBS alone. Stools were assessed from days 8, 11, and 14 for oocyst counts. Mice were killed on day 14, 8 days postinoculation, at the peak of the infection. Ileal and colon segments were obtained for histology, real-time and reverse transcriptase PCR, and immunoassays. Villus and crypt lengths and cross-sectional areas were also measured. Undernourished and nourished mice infected with excysted 10^6 or 10^7 oocysts exhibited the poorest growth outcomes compared with their uninfected controls. Nourished 10^6-infected mice had comparable weight decrements to uninfected undernourished mice. Body weight and villi were additively affected by malnutrition and cryptosporidiosis. Hyperplastic crypts and heavier inflammatory responses were found in the ilea of infected malnourished mice. Undernourished infected mice exhibited greater oocyst shedding, TNF-α and IFN-γ intestinal levels, and mRNA expression compared to nourished mice infected with either 10^5 or 10^6 oocysts. Taken together, these findings show that *Cryptosporidium* infection can cause undernutrition and, conversely, that weanling undernutrition intensifies infection and mucosal damage.

Cryptosporidiosis, first described by Tyzzer (1907) in the gastric glands of infected mice (Tzipori and Ward, 2002), has emerged as an increasingly recognized public health threat. *Cryptosporidium* spp. have been identified in watery diarrhea of patients with HIV and other immunocompromised patients and in large human outbreaks of diarrhea in both developed and developing parts of the world (Harp, 2003; Ramirez et al., 2004; Houpt et al., 2005). Furthermore, the long-term impact of cryptosporidial infection has been increasingly recognized in impoverished settings around the world (Checkley et al., 1997; Guerrant, 1997; Checkley et al., 1998). The wide-range zoonotic potential, resistance to disinfectants, low infectious dose, and easy dissemination upon shedding impressively show how this

*To whom correspondence should be addressed. Center for Global Health, Division of Infectious Diseases and International Health, University of Virginia, Charlottesville, Virginia 22908. rlg9a@virginia.edu.

protozoan is adapted to survive and spread in the environment (Dillingham et al., 2002; Karanis et al., 2007).

Crowded households with inadequate sanitation further aggravate the likelihood of the infection spreading from person to person (Newman et al., 1999; Caccio and Pozio, 2006). The lack of adequate treatment or prevention for high-risk groups for this chlorine-resistant food- and waterborne protozoan adds to the difficulties controlling cryptosporidial infections (Smith and Corcoran, 2004).

Impoverished household environments and water contamination tremendously increase the risk of exposure to waterborne pathogens and the likelihood of oocyst spread. Predisposition to adverse outcomes from repeated or prolonged bouts of diarrhea and enteric infections may additionally have a strong genetic component (Guerrant et al., 2005; Oria et al., 2005, 2007), especially with respect to host–parasite immune interactions.

Longitudinal cohort studies in poor shantytown areas in the developing world by our group and others have highlighted the short- and long-term impact of cryptosporidial infections on growth and development of children (even without overt diarrhea), effects that remain greatly underestimated (Checkley et al., 1997; Guerrant et al., 2005; Savioli et al., 2006; Bushen et al., 2007). In addition, young malnourished children are at greatest risk for developing heavy *Cryptosporidium* spp. infections and likely present the worst outcomes. In crowded household environments, low-birth-weight children were found to be at greater risk for acquiring symptomatic *Cryptosporidium* spp. infection, which, in turn, highlights the vicious cycle of enteric infections and malnutrition leading to increased risk for cryptosporidial infection, malabsorption, and diarrhea during early childhood (Newman et al., 1999).

Undernutrition and enteric illnesses may disrupt the developing immune system (Pallaro et al., 2001; Cunningham-Rundles et al., 2005) against *C. parvum* in growing children, especially in the first 2 yr of life, the same time frame for rapid physical and cognitive development (Guerrant et al., 1999; Niehaus et al., 2002). Therefore, we have focused on a neonatal murine model of cryptosporidiosis to address the interactions of cryptosporidial infection and malnutrition in early life.

Despite worldwide epidemiological data on DALYs (disability-adjusted life years) lost due to enteric infections and undernutrition in early childhood, few studies have addressed the interactions of infection and undernutrition and their effects on postnatal development in well-defined animal models. In the current study, we have investigated the additive effects of *Cryptosporidium* sp. infection with undernutrition in the suckling period in mice, which was found in our model to severely impair normal growth. Furthermore, we find that malnourished mice develop substantially heavier infections and greater mucosal damage than nourished mice given the same inoculum.

MATERIALS AND METHODS

Undernutrition protocol

The protocol described herein is in accordance with the Institutional Animal Care and Use Committee (IACUC) policies of the University of Virginia. Both pregnant and nonpregnant inbred mice (C57BL6J) were purchased from Charles River Laboratories, Inc. (Wilmington, Massachusetts). The pregnant mice were monitored daily before delivery under pathogen-free conditions. Standard chow diet and water were given ad libitum to the dams. After birth, litter size was adjusted to 6–8 pups. Their first day of life was recorded as day 1. Analogous in some ways to weanling undernutrition in impoverished children, the pups

were separated from their lactating dams for increasing intervals starting on day 4 of life. Half of the pups from each litter were separated, starting with 4 hr on day 4, 8 hr on day 5, and 12 hr on day 6 until day 14, according to protocol adapted from Calikoglu et al. (2001). Separated pups were kept in an incubator box under controlled temperature (28 ± 2 C). Nourished controls stayed with their mothers. Litters were kept undisturbed in the first 4 postnatal days to reduce stress and to assure that all pups received initial colostrum. Body weight was recorded daily until mice were killed. A thermal pad was used to warm the pups during daily measurements (28 ± 2 C). Care was taken to keep the same level of animal handling for all groups.

Cryptosporidium parvum infection

On day 6, 1 hr prior to parasite inoculation, pups were separated from their lactating dams to empty their stomachs. Each pup received an oral inoculum of 10^5, 10^6, or 10^7 excysted *C. parvum* oocysts in 10–25 μl of PBS (pH 7.2). Oocysts were obtained from experimentally infected calves (Iowa isolate; Waterborne, Inc., New Orleans, Louisiana). Littermate controls received PBS orally at the same time.

Because excystation rates varied from 20 to 40%, experimental groups were paired to include nourished controls (n = 11) and infected groups given identical inocula at the same time with either 10^5 (n = 14), 10^6 (n = 16), or 10^7 (n = 6) oocysts. Malnourished uninfected controls, (n = 10), and infected mice were given either 10^5 (n = 14), 10^6 (n = 16), or 10^7 (n = 13) oocysts. Due to high mortality rates observed in mice inoculated with the 25 μl of volume required for the 10^7 oocysts, data from the 10^7 dose are only presented for fecal and tissue parasite quantification.

Follow-up

Body weight was measured daily, and stools were collected by gentle stroking of the abdomen. Animals were killed on day 14, 8 days post-inoculum (PI), at the peak of the infection. Animals were anesthetized with sodium pentobarbital, 8 mg/100 g i.p., followed by cervical dislocation. After opening of the abdominal cavity, approximately 1 cm of each middle ileal and colon segments (proximal to the ileocecal valve) were removed without washing, then weighed, divided, and prepared either for histology (24 hr in 10% zinc formalin) or real-time and reverse-transcriptase PCR (frozen immediately in liquid nitrogen and transferred to −80 C). On the day mice were killed, stools were collected before termination or after cervical dislocation, when mice would pass some feces immediately after death. Intestinal sections that had the least amount of fecal material were collected for histology, real-time PCR, and reverse-transcriptase PCR (they were not washed with PBS; 1 cm of tissue was excised). For the mice that had a lot of stool, their intestines were milked to remove feces. Results of *C. parvum* parasites by real-time PCR were expressed in log counts per gram of stool or tissue, respectively.

Morphology analyses

Digital micrographs of intestinal histology were taken with the use of a high-resolution microscope (BH-2, Olympus, Tokyo, Japan), with Photoshop CS software. To address the mucosal villus surface and crypt hyperplastic response, villus height and crypt depth and area were measured with Image J software, at low magnification (×100), from ileum samples at day 14 (8 days PI), following calibration as described elsewhere (Carneiro-Filho et al., 2004). Twenty longitudinal sections of crypts and villi were measured per ileum (n = 4, per group). To perform direct visualization of oocysts, and to confirm infectivity, higher magnifications were used (×400).

Fecal detection of oocyst shedding

A direct immunofluorescence detection procedure was used to confirm infection, according to the manufacturer's instructions (MeriFluor® *Cryptosporidium/Giardia*; Meridian Bioscience, Inc., Cincinnati, Ohio), with the use of FITC labeled anti-*C. parvum* monoclonal antibodies. Stools were collected in a preweighed tube and diluted to 1 mg/25 μl in PBS. Oocysts were detected with the aid of a fluorescence microscope adapted with an image-capturing platform (12-megapixel digital camera) under ×40 magnification. Oocysts were identified by their green color and characteristic size (Bushen et al., 2007).

Real-time PCR protocols

Five microliters of DNA sample was added to 20 μl of master mix (consisting of 12.5 μl of SYBR Green Supermix (BioRad, Hercules, California), 1.0 μl of forward primer, 1.0 of reverse primer, and 5.5 μl of DNAse-, RNAse-free water) to make a total amplification reaction volume of 25 μl. Forward and reverse primers, with the following sequences, 5′-CTGCGAATGGCTCATTATAACA-3′ and 5′-AGGCCAATACCCTACCGTCT-3′, respectively, were used targeting the gene coding for 18s rRNA. Amplification consisted of 15 min at 95 C followed by 40 cycles of 15 sec at 95 C, 30 sec at 60 C, and 30 sec at 70 C. Amplification and detection were performed with the use of the iCycler real-time detection system (iCycler IQ, Biorad). Fluorescence was measured during the annealing step of each cycle. Cycle numbers of each run were compared to a standard curve of known *C. parvum* DNA and transformed into oocyst count per gram of stool sample.

Reverse-transcriptase PCR protocols

Briefly, ileal fragments were immediately immersed and frozen in liquid nitrogen and stored at −80 C until immediately before analyses. Samples were thawed and resuspended in a denaturating solution (4 M guanidinium thiocyanate, 25 mM sodium citrate, pH 7, 0.5% sarcosyl) and extracted with the use of RNeasy mini columns, according to manufacturer's instructions (RNeasy mini kit, Qiagen, Inc., Valencia, California). Total RNA was quantified and checked for purity (A260:280 ratio) by standard spectrophotometry (Biophotometer, Eppendorf, Hamburg, Germany). The first strand of cDNA was synthesized from 2 μg of total RNA with the use of oligo$(dT)_{12–18}$ as primers in the presence of Moloney murine leukemia virus reverse transcriptase (Superscript™ Reverse Transcriptase, Invitrogen, Carlsbad, California), for 1 hr at 37 C. PCR was carried out with 5 μl of the RT product (50 μl final reaction volume) and with 5 μl of reverse and forward murine primers (Invitrogen) for IFN-γ, TNF-α, and IL-10. The following reverse and forward murine primers (Eckmann et al., 1996) were used:

IL-10: 5′-GTGAAGACTTTCTTTCAAACAAAG-3′

5′-CTGCTCCACTGCCTTGCTCTTATT-3′ (274 bp);

IFN-γ: 5′-TGAACGCTACACACTGCATCTTGG-3′

5′-CGACTCCTTTTCCGCTTCCTGAG-3′ (460 bp);

TFN-α: 5′-ATGAGCACAGAAAGCATGATC-3′

5′-TACAGGCTTGTCACTCGAATT-3′ (276 bp); and

β-Actin: 5′-GTGGGCCGCTCTAGGCACCAA-3′

5′-CTCTTTGATGTCACGCACGATTTC-3′ (540 bp).

Amplicons were generated in the thermal cycler (MyCycler, Biorad) conditions. The temperature profile of the amplification consisted of 35 cycles of 15 sec each for denaturation at 95 C, annealing at 55 C and extension at 72 C. Negative controls were run

without RNA. PCR products were separated onto 2% agarose gel and visualized by ethidium bromide staining and photographed digitally with the use of a gel documentation system (Alpha Imager, Alpha Innotech Corp., San Leandro, California). The housekeeping gene, β-actin, was used as an internal control. Sample band densities were ratio-normalized with the use of β-actin band intensities, obtained within the same PCR reaction, with the aid of NIH Image J software (NIH, Bethesda, Maryland).

Immunoassays

Ileal segments were obtained and frozen in liquid nitrogen for TNF-α and IFN-γ immunoassays. PBS containing 0.05% Tween 20 detergent was added to the tissue and left for 10 min on ice before tissue homogenization. Ileal samples were then centrifuged for 5 min, and supernatants were collected for cytokine analyses. Mouse IFN-γ and TNF-α concentrations were measured from ileal homogenates by ELISA kits, with the use of Quantikine-colorimetric sandwich assay (R&D Systems, Inc., Minneapolis, Minnesota), following the manufacturer's protocols.

Statistical analyses

The data analyses and graphs were done with SPSS 14.0 and GraphPad 4.01 for Windows. All statistical analyses were done from raw data with the use of either 1-way ANOVA or Student's *t*-tests where applicable. A *P*-value <0.05 was considered significant. Data are represented as mean ± standard error.

RESULTS

Effects of undernutrition and *Cryptosporidium parvum* infection

Malnourished and nourished mice infected with 10^6 oocysts had impaired weight gain compared with their noninfected controls or with nourished mice infected with 10^5 oocysts (Fig. 1A, B). Nourished mice infected with 10^6 oocysts showed 41% less weight gain compared with uninfected controls ($P < 0.001$) at day 14, 8 days postinfection (PI). Interestingly, nourished 10^6-infected mice have comparable weight decrements to uninfected malnourished mice at the same endpoint. Undernourished mice given 10^6 oocysts had an additional 48% decrement in weight gain at day 14, compared to the average weight gain seen in the uninfected, undernourished controls, thus reaching a full 68% reduction compared with uninfected nourished animals ($P < 0.001$). Therefore, body weight was additively affected by undernutrition and cryptosporidiosis, the latter in an inoculum-load–dependent fashion. Although some animals given 10^7 oocysts died with diarrhea within 1 wk of infection, the few surviving animals provided samples to quantify infection, as shown in Table I.

Intestinal morphology

Ileal morphometry: Cryptosporidium parvum infectivity (10^5 and 10^6 oocysts) caused reductions in villus height in a dose-dependent fashion in both malnourished and nourished infected mice. However, malnourished mice infected with 10^6 oocysts had greater reduction in villus height ($P < 0.05$) compared with infected nourished mice (Fig. 2A).

Crypt depth was found to be significantly greater in the ileum of both nourished and malnourished mice infected with 10^6 oocysts, compared with their respective uninfected controls ($P < 0.05$), showing an adaptive hyperplastic response to the mucosal injury due to the infection. In addition, infection with 10^5 oocysts caused a hyperplastic crypt response in undernourished mice that was not seen with infection at the same dose in nourished animals (Fig. 2B, C).

Representative ileal histology from infected (10^6 oocysts) and uninfected malnourished and nourished mice is shown in Figure 3. Ileal tissue from malnourished uninfected mice showed clear reductions in goblet cell numbers as well as villus blunting compared to the nourished uninfected controls, effects that were even more pronounced in animals with cryptosporidial infection (Fig. 3A). The presence of hyperplastic crypts and villus blunting with cryptosporidial infection was also associated with greater inflammation in the lamina propria, with both neutrophil and eosinophil infiltration. *Cryptosporidium parvum* oocysts were visualized in ileal villus surface epithelium and crypt glands of infected animals (Fig. 3B).

Oocyst counting and shedding

Malnourished mice had >1 log (10-fold) greater fecal oocyst shedding and (except by 0.9 log in the ileum) ileal and colonic tissue infection by quantitative PCR at peak infection on day 14 than nourished siblings given the same infectious doses (either 10^6 or 10^7 oocysts). Malnutrition is associated with a 1.9–2.3 log, i.e., 87–191-fold, heavier infection in the colon and ileum, respectively, with the 10^7-oocyst infectious dose (Table I). At the 10^6-oocyst dose, the differences were 0.9–1.2 log, i.e., 8–16-fold, heavier infection in malnourished animals in the ileum and colon, respectively (Table I). There were no significant differences between nourished and malnourished mice in their time course of shedding.

ELISA immunoassay and reverse-transcriptase PCR

Malnourished mice infected with 10^6 parasites had higher TNF-α levels (picogram/milliliter of ileum tissue) than all the other groups (Fig. 4A), as shown by ELISA immunoassays. Nourished uninfected mice show barely detectable TNF-α mRNA and cytokine levels. Somewhat surprisingly, we found variable and occasionally increased expression of TNF-α mRNA in the ileal specimens examined from uninfected malnourished mice (Fig. 5A). Malnourished mice infected with 10^6 parasites had substantially greater IFN-γ, both by ELISA (Fig. 4B) and mRNA (Fig. 5C), than nourished infected or malnourished uninfected mice ($P < 0.05$). As expected, IFN-γ, mRNA, and cytokine levels were significantly increased in nourished animals infected with 10^6 oocysts (Figs. 4B, 5C). Furthermore, IL-10 mRNA expression was greater in both infected mouse groups as opposed to the uninfected ones. However, its expression was still greater in the ileum of malnourished infected animals (Fig. 5B).

DISCUSSION

The vicious cycle of diarrhea and malnutrition has been recognized as being critical to the staggering cost of child mortality and morbidity in impoverished areas of the world (Guerrant et al., 1992, 2002; Dillingham and Guerrant, 2004). *Cryptosporidium* spp. infections lead to persistent diarrhea and malnutrition, especially in early childhood and in immunocompromised hosts. In patients with AIDS, cryptosporidiosis is associated with severe diarrhea, intestinal mucosal disruption, and potentially with malabsorption of antiretroviral drugs (Brantley et al., 2003; Bushen et al., 2004). Furthermore, cryptosporidial infections during early childhood, even without overt diarrhea, have been associated with long-term growth faltering and cognitive impairment (Checkley et al., 1997; Guerrant et al., 1999).

Weanling undernutrition superimposed upon experimentally induced *C. parvum* infection in neonatal mice provides an excellent model to dissect the components of the vicious infection–malnutrition cycle. This model involves early experimental weaning (maternal

separation), much like the early weaning with consequent heavy diarrhea burdens and malnutrition that occurs in Brazilian shantytown children (Lima et al., 1992).

Novel real-time PCR methods have enabled us to quantify fecal, as well as tissue, parasites, as early as 2 days PI, in both nourished and malnourished experimentally infected mice. We found peak parasite numbers 8 days PI in mice (at 14 days old), a time similar to that found by Ernest et al. (1986) in Swiss Webster mice.

In contrast to Sasahara et al. (2003), we found that *C. parvum*–infected mice, regardless of nutritional status, showed significant decrements in weight gain as early as 2 days PI. This discrepancy is likely because of the inoculum tested. Sasahara et al. (2003) infected suckling mice with only 10^4 oocysts, compared to our infections, which used 10^5 to 10^7 oocysts. Even with lighter doses of oocysts, however, they still observed severe ileal villus blunting.

Undernutrition and *C. parvum* infection were synergistic in disrupting the normal architecture of the ileum. The distal ileum was consistently found to be the predominant site of *C. parvum* colonization and multiplication in suckling mice in our studies, as in those of others (Current and Reese, 1986). Blunted villi and deeper crypts in the ileum were consistently associated with the heavier *C. parvum* burden in the undernourished mice. The addition of undernutrition to *C. parvum* infection in suckling mice approximated the effects of an additional log of oocyst infection in nourished mice. Even with the 10^5 parasite inoculum, the addition of undernutrition increases the effect of deepening mucosal crypts, compared with nourished mice infected with the same oocyst inoculum, suggesting increased cell turnover in response to mucosal epithelial disruption.

In addition, our morphological findings show increased mucosal inflammatory changes and leukocyte recruitment in the ileum of *C. parvum*–infected mice, particularly the ones subjected to undernutrition. High levels of IFN-γ and TNF-α (as we found in the ileal tissues from undernourished infected mice), have been recently implicated in intestinal barrier dysfunction and enterocyte apoptosis (Begue et al., 2006; Wang et al., 2006), and correlate with the degree of inflammatory response seen with heavy infection (Buret et al., 2003). Interestingly, severe undernutrition is also reported to elevate proinflammatory cytokines in children (Dulger et al., 2002).

IFN-γ is a well-recognized factor in the Th-1 cell-mediated response against *C. parvum* infections. Increased expression of IFN-γ has been found following *C. parvum* challenge (Deng et al., 2004). Furthermore, in the absence of IFN-γ, TNF-α expression in the infected intestinal mucosa is significantly decreased. TNF-α has been shown to reduce oocyst shedding, via NF-κp upregulation (Lacroix et al., 2001; Lean et al., 2002). Hence, the increased IFN-γ and TNF-α seen with heavier cryptosporidial infections in our malnourished mice may either be blunted or rendered less effective by yet unknown mechanisms.

Interestingly, although micronutrient and vitamin deficiencies, such as zinc or vitamin A depletion (Prasad, 2000; Wieringa et al., 2004), are believed to impair adaptive and innate immune responses, malnourished infected mice did not show immune cytokine suppression; conversely, these animals showed a strong proinflammatory response, which might have accentuated the mucosal damage due to the malnutrition challenge. However, the effects of specific micronutrients on immunity following enteric infections are not well understood (Hughes and Kelly, 2006) and were not addressed in these studies.

Nutritional impairments may reduce immune-cell mass and indirectly affect immune function, particularly T helper cells (Fraker et al., 2000). Lymphopenia and thymic atrophy, which can be found in zinc deficiency, are now known to be due to loss of precursor T and B cells in the bone marrow (Thurnham, 1997). Additionally, T and B cell reductions may be

aggravated by premature weaning, due to reduced maternal-milk–derived lymphocytes being transferred to the pups (Flo et al., 1994). Deprivation of critical nutrients, lymphocytes, and maternal antibodies provided by full breast feeding might explain why higher intestinal levels of IFN-γ and TNF-α in malnourished infected mice were not sufficient to reduce the intensity of cryptosporidial infections.

Alcantara et al. (2003) found increased stool TNF-α and lactoferrin (a marker of neutrophilic inflammation) levels in Brazilian children with cryptosporidiosis. Kirkpatrick et al. (2002) also found that cryptosporidiosis stimulates intestinal inflammation in malnourished Haitian children, with predominant Th2 cytokine response and increased IL-10, but not IFN-γ. This suggests a counterregulatory role of IL-10 in blocking the Th1-mediated overresponse seen in malnourished and heavy infected ilea. However, IL-10 expression might also be considered a feature of ongoing immune responses against infectious pathogens (Mocellin et al., 2004). In our animal model, we also see increased IL-10 mRNA, especially in the infected ileum in weanling malnourished animals. However, this occurred without absolute suppression of Th-1-mediated responses, as seen by higher levels of IFN-γ secretion (detected by ELISA) and also RNA transcription (detected by reverse-transcriptase PCR). It remains possible that these higher levels of IFN-γ represent relative suppression of levels that might otherwise have been even higher with the heavier intensity of infection. Undernutrition and poor weight gain (low fat mass) may also impair immune responses by reducing leptin levels. Leptin typically polarizes Th cells toward a Th1 phenotype (Faggioni et al., 2001).

In summary, undernutrition along with cryptosporidiosis causes mucosal disruption, reduced absorptive surface, and increased proinflammatory cytokine responses, leading to growth impairment. Furthermore, the intensity of the inflammatory response and mucosal disruption parallel the burden of *C. parvum* infection.

Neonatal mice provide a model to demonstrate both the effect of cryptosporidial infection on growth impairment and the effect of weanling undernutrition on increased susceptibility to intensified infection. This model allows the dissection of the components of infection and malnutrition in the “vicious cycle” that now enables further study of mechanisms and potential interventions to help break this cycle that is so devastating to children's health and development.

Acknowledgments

This research was supported by NIH Cooperative Agreement U54 AI57168 for the Mid-Atlantic Regional Center for Excellence (MARCE) funded by the National Institute of Allergy and Infectious Diseases, and by Fogarty International Center grant TW006713-01. Bruna P. Coutinho was supported in part by the Brazilian CAPES agency and the Fund for the Improvement of Postsecondary Education (FIPSE) from the United States–Brazil Higher Education Consortium Program and, with Dr. Carlos Vieira, by the Fogarty International Center Global Infectious Diseases Research Training (GIDRT) program at NIH, grant D43 TW006578. Dr. Jesus Emmanuel Sevilleja was supported by the Ellison Medical Foundation, grant ID-T-0019-03, and the Pfizer Initiative in International Health at the University of Virginia.

LITERATURE CITED

Alcantara CS, Yang CH, Steiner TS, Barrett LJ, Lima AAM, Chappell CL, Okhuysen PC, White AC JR. Guerrant RL. Interleukin-8, tumor necrosis factor-alpha, and lactoferrin in immunocompetent hosts with experimental and Brazilian children with acquired cryptosporidiosis. The American Journal of Tropical Medicine and Hygiene. 2003; 68:325–328. [PubMed: 12685639]

Begue B, Wajant H, Bambou JC, Dubuquoy L, Siegmund D, Beaulieu JF, Canioni D, Berrebi D, Brousse N, Desreumaux P, et al. Implication of TNF-related apoptosis-inducing ligand in

inflammatory intestinal epithelial lesions. Gastroenterology. 2006; 130:1962–1974. [PubMed: 16762619]

Brantley RK, Williams KR, Silva TM, Sistrom M, Thielman NM, Ward H, Lima AA, Guerrant RL. AIDS-associated diarrhea and wasting in Northeast Brazil is associated with subtherapeutic plasma levels of antiretroviral medications and with both bovine and human subtypes of *Cryptosporidium parvum*. Brazilian Journal of Infectious Disease. 2003; 7:16–22.

Buret AG, Chin AC, Scott KGE. Infection of human and bovine epithelial cells with *Cryptosporidium andersoni* induces apoptosis and disrupts tight junctional ZO-1: Effects of epidermal growth factor. International Journal of Parasitology. 2003; 33:1363–1371. [PubMed: 14527519]

Bushen OY, Davenport JA, Lima AB, Piscitelli SC, Uzgiris AJ, Silva TMJ, Leite R, Kosek M, Dillingham RA, Girao A, Lima AAM, Guerrant RL. Diarrhea and reduced levels of antiretroviral drugs: Improvement with glutamine or alanyl-glutamine in a randomized controlled trial in northeast Brazil. Clinical Infectious Diseases. 2004; 38:1764–1770. [PubMed: 15227625]

Bushen OY, Kohli A, Pinkerton RC, Dupnik K, Newman RD, Sears CL, Fayer R, Lima AAM, Guerrant RL. Heavy cryptosporidial infections in children in northeast Brazil: Comparison of *Cryptosporidium hominis* and *Cryptosporidium parvum*. Transactions of the Royal Society of Tropical Medicine and Hygiene. 2007; 101:378–384. [PubMed: 16934303]

Caccio SM, Pozio E. Advances in the epidemiology, diagnosis and treatment of cryptosporidiosis. Expert Review of Anti-Infective Therapy. 2006; 4:429–443. [PubMed: 16771620]

Calikoglu A, Karayal A, D'Ercole A. Nutritional regulation of IGF-I expression during brain development in mice. Pediatric Research. 2001; 49:197–202. [PubMed: 11158513]

Carneiro-Filho BA, Oria RB, Wood RK, Brito GA, Fujii J, Obrig T, Lima AA, Guerrant RL. Alanyl-glutamine hastens morphologic recovery from 5-fluorouracil-induced mucositis in mice. Nutrition. 2004; 20:934–941. [PubMed: 15474885]

Checkley W, Gilman RH, Epstein LD, Suarez M, Diaz JF, Cabrera L, Black RE, Sterling CR. Asymptomatic and symptomatic cryptosporidiosis: Their acute effect on weight gain in Peruvian children. American Journal of Epidemiology. 1997; 145:156–163. [PubMed: 9006312]

Checkley W, Epstein LD, Gilman RH, Black RE, Cabrera L, Sterling CR. Effects of *Cryptosporidium parvum* infection in Peruvian children: Growth faltering and subsequent catch-up growth. American Journal of Epidemiology. 1998; 148:497–506. [PubMed: 9737562]

Cunningham-Rundles S, McNeeley DF, Moon A. Mechanisms of nutrient modulation of the immune response. The Journal of Allergy and Clinical Immunology. 2005; 115:1119–1128. [PubMed: 15940121]

Current WL, Reese NC. A comparison of endogenous development of three isolates of *Cryptosporidium* in suckling mice. The Journal of Protozoology. 1986; 33:98–108. [PubMed: 3959014]

Deng M, Rutherford MS, Abrahamsen MS. Host intestinal epithelial response to *Cryptosporidium parvum*. Advanced Drug Delivery Reviews. 2004; 56:869–884. [PubMed: 15063595]

Dillingham RA, Guerrant RL. Childhood stunting: Measuring and stemming the staggering costs of inadequate water and sanitation. Lancet. 2004; 363:94–95. [PubMed: 14726158]

Dillingham RA, Lima AA, Guerrant RL. Cryptosporidiosis: Epidemiology and impact. Microbes and Infection. 2002; 4:1059–1066. [PubMed: 12191656]

Dulger H, Arik M, Sekeroglu MR, Tarakcioglu M, Noyan T, Cesur Y, Balahoroglu R. Pro-inflammatory cytokines in Turkish children with protein-energy malnutrition. Mediators of Inflammation. 2002; 11:363–365. [PubMed: 12581501]

Eckmann L, Fierer J, Kagnoff MF. Genetically resistant (Ityr) and susceptible (Itys) congenic mouse strains show similar cytokine responses following infection with *Salmonella dublin*. Journal of Immunology. 1996; 156:2894–2900.

Ernest JA, Blagburn BL, Lindsay DS, Current WL. Infection dynamics of *Cryptosporidium parvum* (Apicomplexa: Cryptosporidiae) in neonatal mice (*Mus musculus*). Journal of Parasitology. 1986; 72:796–798. [PubMed: 3806334]

Faggioni R, Feingold KR, Grunfeld C. Leptin regulation of the immune response and the immunodeficiency of malnutrition. FASEB Journal. 2001; 15:2565–2571. [PubMed: 11726531]

Flo J, Elias F, Massouh E, Roux ME. Impairment of B and T cell maturation in gut associated lymphoid tissues due to malnutrition during lactation. Developmental and Comparative Immunology. 1994; 18:543–555. [PubMed: 7768319]

Fraker PJ, King LE, Laakko T, Vollmer TL. The dynamic link between the integrity of the immune system and zinc status. Journal of Nutrition. 2000; 130:1399S–1406S. [PubMed: 10801951]

Guerrant DI, Moore SR, Lima AA, Patrick PD, Schorling JB, Guerrant RL. Association of early childhood diarrhea and cryptosporidiosis with impaired physical fitness and cognitive function four—seven years later in a poor urban community in northeast Brazil. The American Journal of Tropical Medicine and Hygiene. 1999; 61:707–713. [PubMed: 10586898]

Guerrant RL. Cryptosporidiosis: An emerging, highly infectious threat. Emerging Infectious Diseases. 1997; 3:51–57. [PubMed: 9126444]

Guerrant RL, Kosek M, Moore S, Lorntz B, Brantley R, Lima AA. Magnitude and impact of diarrheal diseases. Archives of Medical Research. 2002; 33:351–355. [PubMed: 12234524]

Guerrant RL, Oria R, Bushen OY, Patrick PD, Huopt E, Lima AA. Global impact of diarrheal diseases that are sampled by travelers: The rest of the hippopotamus. Clinical Infectious Diseases. 2005; 41(Suppl. 8):S524–S530. [PubMed: 16267713]

Guerrant RL, Schorling JB, Mcauliffe JF, de SOUZA MA. Diarrhea as a cause and effect of malnutrition: Diarrhea prevents catch-up growth and malnutrition increases diarrhea frequency and duration. The American Journal of Tropical Medicine and Hygiene. 1992; 47(Suppl.):28–35. [PubMed: 1632474]

Harp JA. *Cryptosporidium* and host resistance: Historical perspective and some novel approaches. Animal Health Research Reviews. 2003; 4:53–62. [PubMed: 12885209]

Houpt ER, Bushen OY, Sam NE, Kohli A, Asgharpour A, Ng CT, Calfee DP, Guerrant RL, Maro V, Ole-Nguyaine S, Shao JF. Short report: Asymptomatic *Cryptosporidium hominis* infection among human immunodeficiency virus-infected patients in Tanzania. The American Journal of Tropical Medicine and Hygiene. 2005; 73:520–522. [PubMed: 16172475]

Hughes S, Kelly P. Interactions of malnutrition and immune impairment, with specific reference to immunity against parasites. Parasite Immunology. 2006; 28:577–588. [PubMed: 17042929]

Karanis P, Kourenti C, Smith H. Waterborne transmission of protozoan parasites: A worldwide review of outbreaks and lessons learnt. Journal of Water and Health. 2007; 5:1–38. [PubMed: 17402277]

Kirkpatrick BD, Daniels MM, Jean SS, Pape JW, Karp C, Littenberg B, Fitzgerald DW, Lederman HM, Nataro JP, Sears CL. Cryptosporidiosis stimulates an inflammatory intestinal response in malnourished Haitian children. The Journal of Infectious Diseases. 2002; 186:94–101. [PubMed: 12089667]

Lacroix S, Mancassola R, Naciri M, Laurent F. *Cryptosporidium parvum*-specific mucosal immune response in C57BL/6 neonatal and gamma interferon-deficient mice: Role of tumor necrosis factor alpha in protection. Infection and Immunity. 2001; 69:1635–1642. [PubMed: 11179338]

Lean IS, McDonald V, Pollok RC. The role of cytokines in the pathogenesis of *Cryptosporidium* infection. Current Opinion in Infectious Diseases. 2002; 15:229–234. [PubMed: 12015455]

Lima AA, Fang G, Schorling JB, de Albuquerque L, Mc-Auliffe JF, Mota S, Leite R, Guerrant RL. Persistent diarrhea in Northeast Brazil: Etiologies and interactions with malnutrition. Acta Paediatrica. 1992; 81(Suppl. 381):S39–S44.

Mocellin S, Marincola F, Rossi CR, Nitti D, Lise M. The multifaceted relationship between IL-10 and adaptive immunity: Putting together the pieces of the puzzle. Cytokine & Growth Factor Reviews. 2004; 15:61–76. [PubMed: 14746814]

Newman RD, Sears CL, Moore SR, Nataro JP, Wuhib T, Agnew DA, Guerrant RL, Lima AA. Longitudinal study of *Cryptosporidium* infection in children in northeastern Brazil. The Journal of Infectious Diseases. 1999; 180:167–175. [PubMed: 10353875]

Niehaus MD, Moore SR, Patrick PD, Derr LL, Lorntz B, Lima AA, Guerrant RL. Early childhood diarrhea is associated with diminished cognitive function 4 to 7 years later in children in a northeast Brazilian shantytown. The American Journal of Tropical Medicine and Hygiene. 2002; 66:590–593. [PubMed: 12201596]

Oria RB, Patrick PD, Blackman JA, Lima AA, Guerrant RL. Role of apolipoprotein E4 in protecting children against early childhood diarrhea outcomes and implications for later development. Medical Hypotheses. 2007; 68:1099–10107. [PubMed: 17098371]

Oria RB, Patrick PD, Zhang H, Lorntz B, Castro-Costa CM, Brito GA, Barrett LJ, Lima AA, Guerrant RL. APOE4 protects the cognitive development in children with heavy diarrhea burdens in northeast Brazil. Pediatric Research. 2005; 57:310–316. [PubMed: 15611352]

Pallaro AN, Roux ME, Slobodianik NH. Nutrition disorders and immunologic parameters: Study of the thymus in growing rats. Nutrition. 2001; 17:724–728. [PubMed: 11527659]

Prasad AS. Effects of zinc deficiency on Th1 and Th2 cytokine shifts. The Journal of Infectious Diseases. 2000; 182(Suppl. 1):S62–S68. [PubMed: 10944485]

Ramirez NE, Ward LA, Sreevatsan S. A review of the biology and epidemiology of cryptosporidiosis in humans and animals. Microbes and Infection. 2004; 6:773–785. [PubMed: 15207825]

Sasahara T, Maruyama H, Aoki M, Kikuno R, Sekiguchi T, Takahashi A, Satoh Y, Kitasato H, Takayama Y, Inoue M. Apoptosis of intestinal crypt epithelium after *Cryptosporidium parvum* infection. Journal of Infection and Chemotherapy. 2003; 9:278–281. [PubMed: 14513402]

Savioli L, Smith H, Thompson A. Giardia and *Cryptosporidium* join the “Neglected Diseases Initiative.”. Trends in Parasitology. 2006; 22:203–208. [PubMed: 16545611]

Smith HV, Corcoran GD. New drugs and treatment for cryptosporidiosis. Current Opinion in Infectious Diseases. 2004; 17:557–564. [PubMed: 15640710]

Thurnham DI. Micronutrients and immune function: Some recent developments. Journal of Clinical Pathology. 1997; 50:887–891. [PubMed: 9462235]

Tyzzer EE. A sporozoan found in the peptic glands of the common mouse. Proceedings of the Society for Experimental Biology and Medicine. 1907; 5:12–13.

Tzipori S, Ward H. Cryptosporidiosis: Biology, pathogenesis and disease. Microbes and Infection. 2002; 4:1047–1058. [PubMed: 12191655]

Wang F, Schwarz BT, Graham WV, Wang Y, Su L, Clayburgh DR, Abraham C, Turner JR. IFN-gamma-induced TNFR2 expression is required for TNF-dependent intestinal epithelial barrier dysfunction. Gastroenterology. 2006; 131:1153–1163. [PubMed: 17030185]

Wieringa FT, Dijkhuizen MA, West CE, van der Ven-Jongekrijg J, Muhilal, van der Meer JWM. Reduced production of immunoregulatory cytokines in vitamin A- and zinc-deficient Indonesian infants. European Journal of Clinical Nutrition. 2004; 58:1498–1504. [PubMed: 15162133]

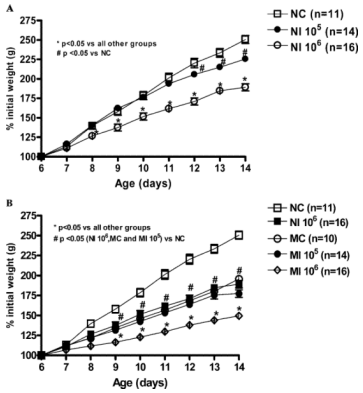

Figure 1.

Body weight gain (% initial weight) from the experimental groups starting the day of *C. parvum* inoculation at day 6 until day 14 (8 days PI). (**A**) Nourished controls (NC, n = 11) are compared with nourished infected (NI) groups given 10^5, n = 14; or 10^6 oocysts, n = 16. (**B**) Malnourished uninfected controls (MC), n = 10, and malnourished infected mice (MI) treated with 10^6, n = 16; or 10^5, n = 14, oocysts. Statistical analyses were done from raw data with the use of ANOVA. The significance level was set at $P < 0.05$. The results are shown as mean ± SEM.

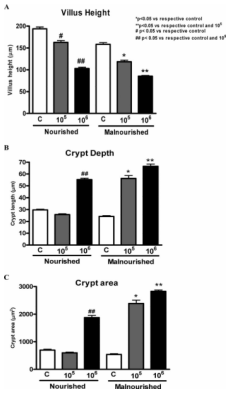

Figure 2.

Morphometric analyses of villus height (**A**), crypt depth (**B**), and (**C**) crypt area from *C. parvum*-infected and uninfected mice (n = 4 for each group). Statistical analyses were done from raw data with the use of ANOVA. The significance level was set at $P < 0.05$. C = uninfected control, 10^5 = inoculum with 10^5 oocysts; 10^6 = inoculum with 10^6 oocysts.

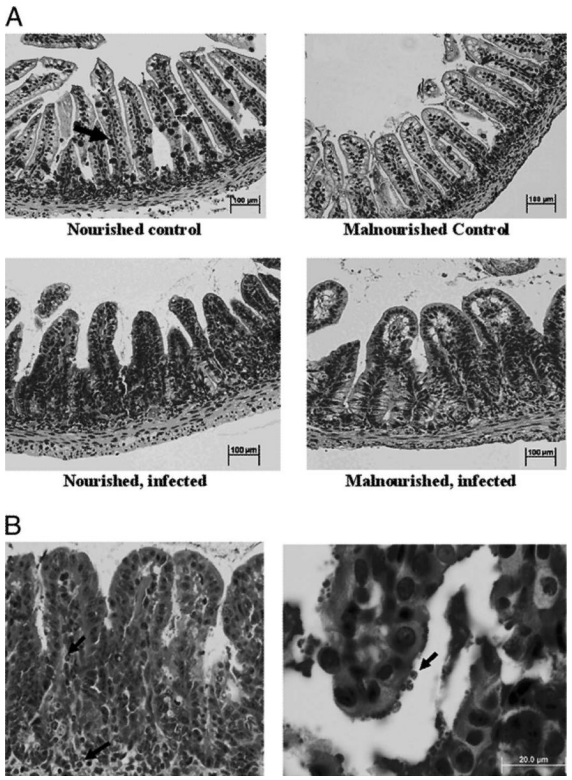

Figure 3.

(**A**) Ileal histology (H&E ×100) in nourished and under-nourished control and infected 14-day-old mice. Note reduction in goblet cell numbers in the infected ileum as compared with the nourished unchallenged control (arrow). (**B**) Details of ileal histology from malnourished mice infected with 10^6 oocysts. On the left, note villus blunting, hyperplasic crypts, and neutrophil and eosinophil infiltration (arrows), H&E ×200. On the right, high-power magnification of a selected villus, showing cryptosporidial parasites at the enterocyte apical surface (arrow), H&E ×400.

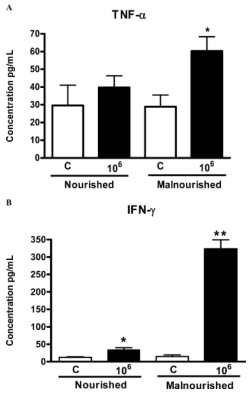

Figure 4.

Tumor necrosis factor-alpha (TNF-α) (**A**) and interferon-gamma (IFN-γ) (**B**) concentrations from frozen ileal segments. Mouse IFN-γ and TNF-α concentrations were measured in ileal homogenates by ELISA. Statistical analyses were done with raw data (Student's *t*-test). The results are shown as mean ±SEM. (**C**) Noninfected control (n = 5, for both nourished and undernourished mice); 10^6 = inoculum with 10^6 oocysts (n = 6, for both nourished and undernourished mice). An asterisk indicates $P < 0.05$ versus respective control.

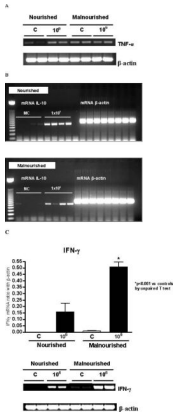

Figure 5.

RT-PCR analysis on (**A**) tumor necrosis factor-alpha (TNF-α) and (**B**) interleukin-10 (IL-10) mRNA expression in the distal ileum (n = 4 for each group) from day 14 (8 days PI) in infected (1×10^6 *C. parvum* oocysts) and noninfected control mice, according to nutritional status. (**C**) Interferon-gamma (IFN-γ) mRNA expression in the distal ileum in infected (1×10^6 *C. parvum* oocysts) and noninfected control at day 14, according to nutritional status. The results are shown as mean ± SEM; **P* < 0.05.

Table I

Log counts of *C. parvum* parasites in the ileum, colon, and stools, as determined by quantitative real-time PCR (qRT-PCR).*

Source	Day of life	Oocyst dose	Nourished	N	Undernourished	N	*P* value
Ileum tissue homogenate	14	10^6	3.23 ± 0.23	6	4.13 ± 0.44	7	0.107
		10^7	2.74 ± 0.13	3	5.02 ± 0.11	6	<0.001
Colon tissue homogenate	14	10^6	4.13 ± 0.18	11	5.29 ± 0.44	11	0.024
		10^7	2.85 ± 0.11	3	4.79 ± 0.25	7	0.001
Stool dilution	14	10^6	3.53 ± 0.26	14	4.55 ± 0.28	12	0.012

*Results are shown in a log scale as mean ± SEM. Data were analyzed with the use of the Student's *t* test. *Cryptosporidium parvum* infection in the ileum, colon, and shedding in stools was determined by qRT-PCR. qRT-PCR data were expressed per gram of stool or tissue.